Available online at www.sciencedirect.com
SCIENCE DIRECT®
Journal of Solid State Chemistry 179 (2006) 486–491
JOURNAL OF SOLID STATE CHEMISTRY
www.elsevier.com/locate/jssc

Magnetic study of two isotypic manganese chloro-sulfides: $MnSbS_2Cl$ and the new compound $MnBiS_2Cl$

Charlotte Doussier[a,*], Gilles André[b], Philippe Léone[a], Etienne Janod[a], Yves Moëlo[a]

[a]*Laboratoire de Chimie des Solides, Institut des Matériaux Jean Rouxel, UMR 6502 CNRS-Université de Nantes, 2 rue de la Houssinière, BP 32229, 44322 Nantes Cedex 03, France*

[b]*Laboratoire Léon Brillouin, CEA-CNRS, CEA-Saclay, 91191 Gif-sur-Yvette Cedex, France*

Received 2 September 2005; received in revised form 27 October 2005; accepted 30 October 2005
Available online 15 December 2005

Abstract

Among the $MnPnQ_2X$ compounds (*Pn*: pnictide; *Q*: chalcogen; *X*: halogen), two isotypic chloro-sulfides, $MnSbS_2Cl$ and $MnBiS_2Cl$, have been studied. $MnBiS_2Cl$ is a new compound synthesized by solid state reaction at 500 °C. It is orthorhombic, space group *Pnma*, with $a = 9.502(2)$, $b = 3.8802(8)$, $c = 12.305(3)$ Å, $V = 453.7(2)$ Å^3, $Z = 4$. Its X-ray single crystal study shows (001) waved layers of MnS_4Cl_2 octahedra, opposite edge-sharing along *b*, and corner-sharing along *a*. Similar magnetic susceptibilities for both compounds have been recorded, indicating high spin Mn^{2+} with anti-ferromagnetic exchange. Correlatively, specific heat versus temperature shows a magnetic transition at $T_N = 35$ K for the Sb-bearing compound, and a two-steps magnetic transition at 28 and 32 K for the Bi isotype. The magnetic structure of $MnSbS_2Cl$ has been determined by neutron diffraction, revealing a magnetic ordering at 1.5 K with an incommensurate wave-vector along *b* ($k = [0, 0.3838, 0]$). Two modulation models, sinusoidal and helicoidal, give quite equivalent reliability factors ($R_{mag} = 0.0573$ and 0.0586, respectively).
© 2005 Elsevier Inc. All rights reserved.

Keywords: Chloro-sulfide; Manganese; Anti-ferromagnetism; Neutron diffraction; Magnetic structure; Incommensurate modulation

1. Introduction

Relatively to chalcogenides or halogenides, mixed compounds of the halogeno-chalcogenide type have been poorly studied up to now. Among them, quaternary compounds combining a transition metal TM with another cation are of special interest for their physical properties, due to the dilution of TM in the crystal matrix and the competition of the two types of cations versus the two ligands. The most frequent case is the combination of Cu, secondly Ag or others transition metals like Cd, Hg and In, with a pnictide *Pn* (*Pn* = P, As, Sb, Bi) [1]. Recently, several compounds implying Mn were synthesized. All correspond to the general formula $TMPnQ_2X$ (*Q*: chalcogen; *X*: halogen). The first compound, $MnSbSe_2I$ [2], is monoclinic, space group $C2/m$. Pfitzner et al. [3] described the isotypic compound $MnBiSe_2I$ and mentioned the synthesis of $MnBiS_2Br$, also as an isotype. On the contrary, $MnSbS_2Cl$ [4] is orthorhombic, space group *Pnma*. All these compounds with divalent manganese are interesting for their magnetic properties. For this purpose, we present here the synthesis and the crystal structure of the new compound $MnBiS_2Cl$, and the magnetic susceptibilities and specific heat of these both compounds. Neutron diffraction permitted to reveal the modulated magnetic structure of $MnSbS_2Cl$.

2. Experimental section

2.1. Synthesis and initial characterization of $MnBiS_2Cl$

$MnBiS_2Cl$ was synthesized by solid state reaction of stoichiometric amounts of MnS, $MnCl_2$ and Bi_2S_3 (1:1:1). The starting materials were homogenized by grinding, put into a sealed evacuated silica tube and heated at 500 °C for 10 days. The final product was characterized by powder X-ray diffraction (Siemens D5000, Cu $K\alpha_1$, $\lambda = 1.5406$ Å).

*Corresponding author. Fax: +33 2 40 37 39 95.
E-mail address: charlotte.doussier@cnrs-imn.fr (C. Doussier).

0022-4596/$ - see front matter © 2005 Elsevier Inc. All rights reserved.
doi:10.1016/j.jssc.2005.10.045

Some powder was included in epoxy and prepared as a polished section to permit its examination with scanning electron microscope equipped with energy dispersive spectrometer (SEM-EDS analysis). The measured atomic percentages were Mn:Bi:S:Cl≈0.96:0.90:2.00:1.04 (averaged experimental data), in agreement with the ideal ratio 1:1:2:1.

2.2. Crystal structure determination of $MnBiS_2Cl$

Some purple needles were observed in the massive powder. Among them, one single crystal of $MnBiS_2Cl$ was glued on the top of a glass capillary and mounted on a STOE-IPDS single φ axis diffractometer using Mo $K\alpha$ radiation ($\lambda = 0.71073$ Å). The exposure time was 2 min·plate^{-1}, φ varying from 0° to 360° with an increment of 1°. The crystal-to-detector distance was set to 35 mm ($\theta_{max} = 34.97°$). The images were processed with a set of STOE programs. Crystal structure was solved in the space group *Pnma* (No. 62) using direct methods (SHELXL-97 software) [5] for heavy atoms (Mn, Bi), and Fourier difference series for other ones. All atoms were refined with anisotropic displacement parameters. Absorption corrections were applied on account of the presence of bismuth atoms. The final refinement converged to a reliability factor $R = 0.0368$ for all data. Crystallographic data and results of the structure refinement are compiled in Table 1. Atomic coordinates are given in Table 2, and the list of anisotropic displacement parameters for all atoms in Table 3.

Table 1
Crystallographic data for the X-ray structure determination of $MnBiS_2Cl$

Compound	$MnBiS_2Cl$
Formula weight, g mol^{-1}	363.49
Crystal system	Orthorhombic
Space group	*Pnma* (No. 62)
Crystal size, mm^3	$0.14 \times 0.01 \times 0.01$
Colour/shape	Purple/needle
a, Å	9.502(2)
b, Å	3.8802(8)
c, Å	12.305(3)
V, Å^3	453.69(16)
Z	4
$F(000)$	628
D_{calc}, g cm^{-3}	5.322
μ, mm^{-1}	42.82
T, K	293(2)
θ_{max}, °	30.00
hkl value	$-13 \leqslant h \leqslant 13$ $-5 \leqslant k \leqslant 4$ $-16 \leqslant l \leqslant 17$
No. reflections; R_{int}	6819; 0.0792
No. independent reflections (obs; all)	647; 754
No. refined parameters	32
R_1 ($I \geqslant 2\sigma$ (I); all)	0.0274; 0.0368
wR_2 ($I \geqslant 2\sigma$ (I); all)	0.0607; 0.0615
GooF	1.180
Residual electronic density, e Å^{-3}	3.257 and −2.072

Table 2
Atomic coordinates and equivalent isotropic displacement parameters for $MnBiS_2Cl$

Atom		x	y	z	U_{eq}, Å^2
Bi	4c	0.6976(1)	0.25	0.5327(1)	0.0156(2)
Mn	4c	0.0069(1)	0.75	0.7370(1)	0.0158(3)
S1	4c	0.7516(2)	0.75	0.6775(2)	0.0135(4)
S2	4c	0.4503(2)	0.25	0.6178(2)	0.0128(4)
Cl	4c	0.0670(2)	0.25	0.6109(2)	0.0173(4)

Table 3
Anisotropic displacement parameters U^{ij} (Å^2) for $MnBiS_2Cl$

Atom	U^{11}	U^{22}	U^{33}	U^{12}	U^{13}	U^{23}
Bi	0.015(1)	0.015(1)	0.017(1)	0.0	−0.002(1)	0.0
Mn	0.015(1)	0.016(1)	0.016(1)	0.0	−0.002(1)	0.0
S1	0.011(1)	0.015(1)	0.015(1)	0.0	0.001(1)	0.0
S2	0.012(1)	0.015(1)	0.012(1)	0.0	0.001(1)	0.0
Cl	0.020(1)	0.016(1)	0.016(1)	0.0	−0.003(1)	0.0

2.3. Magnetic measurements, specific heat and neutron diffraction

Magnetic measurements were carried out on a Quantum Design SQUID magnetometer using powder. The magnetization was measured in the temperature range 2–300 K under 100 Oe applied field. The data were corrected for the sample holder contribution and the core diamagnetism using the Pascal's constants.

Calorimetric measurements were performed on a home-made specific heat setup using the semi-adiabatic method in the temperature range 5–60 K. Data recorded on sintered pellets were corrected for the sample holder and grease contributions.

Powder neutron diffraction experiments were performed at the Laboratoire Léon Brillouin (CEA-CNRS) in Saclay. The high-flux multi-detector (800 cells) of the G4.1 diffractometer ($\lambda = 2.4266$ Å) was used for the determination of the magnetic structure of $MnSbS_2Cl$ and the thermal evolution of the low temperature patterns. Fourteen diagrams were collected between 1.5 and 51 K in the 2θ range 13–93°. The magnetic structure was refined using the Rietveld [6] Fullprof [7] software. The nuclear scattering lengths and manganese magnetic form factor were those included in this program.

3. Results and discussion

3.1. Crystal structure of $MnBiS_2Cl$

$MnBiS_2Cl$ is isotypic with $MnSbS_2Cl$ [4], with unit cell parameters $a = 9.502$ (resp. 9.535), $b = 3.8802$ (resp. 3.8159), $c = 12.305$ (resp. 12.245) Å, $V = 453.68$ (resp. 445.53) Å^3, $Z = 4$. Its structure can be described as

edge-sharing MnS_4Cl_2 octahedra along the *b*-axis, and corner-sharing along the *a*-axis, forming waved layers separated by bismuth atoms (Fig. 1). The chlorine atoms positions have been confirmed by bond valence calculations [8] and neutron diffraction measurements. Bi atoms are located within a distorted bi-capped trigonal prism (5 S + 3 Cl), with close bonding with S atoms exclusively in a dissymmetric square-pyramidal coordination (Fig. 2). Bi^{3+} cation being larger than Sb^{3+} one, the cell volume increases with Bi, although the *a* parameter decreases. This can be explained by considering the effect of the stereochemical activity of lone electron pair of pnictides [9]. This effect is more important for Sb atoms which adopt a more dissymmetric environment than Bi atoms. The distance of the Cl atoms in the coordination sphere of Sb has as a consequence a stretching of Mn chains along the *a*-axis. $MnSbS_2Cl$ and $MnBiS_2Cl$ have not the same structure than $MnSbSe_2I$ [2] and $MnBiSe_2I$ [3]. The comparison between crystal structures is illustrated in Fig. 3. In Cl-bearing compounds, there is only one type of octahedra [MnS_4Cl_2], while, in I-bearing compounds, Mn atoms present two octahedral environments [$MnSe_6$] and [$MnSe_2I_4$], due to the segregation of iodine atoms.

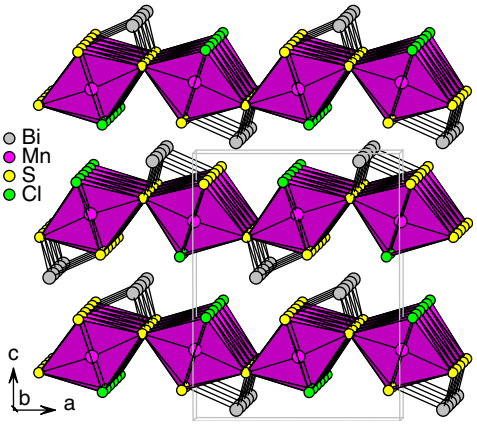

Fig. 1. Crystal structure of $MnBiS_2Cl$.

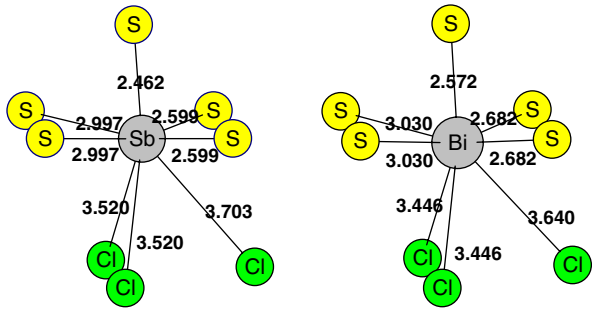

Fig. 2. Bi-capped trigonal prismatic environments of Sb and Bi atoms in $MnSbS_2Cl$ (left) and $MnBiS_2Cl$ (right). (Inter-atomic distances are in Å.)

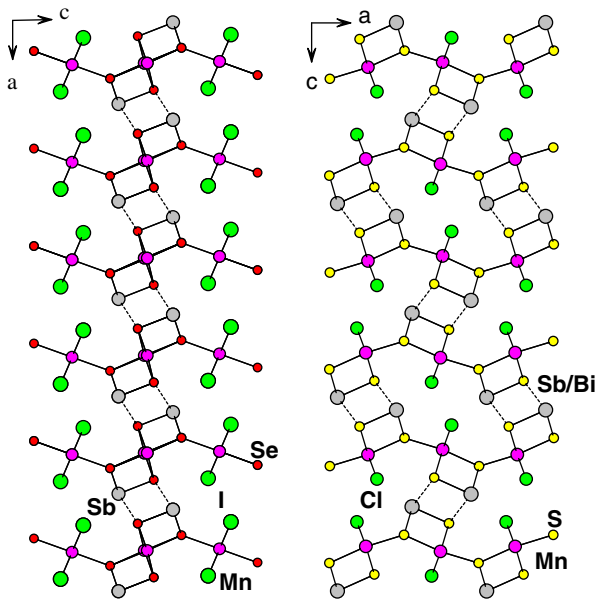

Fig. 3. Comparison of the crystal structures of $MnSbSe_2I$ (left) and $Mn(Sb/Bi)S_2Cl$ (right); projected along the *b*-axis.

3.2. Magnetic susceptibility and specific heat

The magnetic susceptibility versus temperature, recorded at $H = 100$ Oe for both compounds, and the inverse of the magnetic susceptibility in function of temperature, are given in Fig. 4. Magnetic data of $MnSbS_2Cl$ are those of a preceding article [4]. The two types of curve are very similar. The high-temperature data obey the Curie–Weiss law: $\chi^{-1} = (T-\theta)/C$ (insert in Fig. 4). In fitting curves of the inverse of magnetic susceptibility, Curie temperatures θ have been evaluated at around -128 K for $MnSbS_2Cl$ and -120 K for $MnBiS_2Cl$. Negative values for θ are characteristic of anti-ferromagnetic exchange interactions. The calculated effective magnetic moments of manganese atoms are $\mu_{eff} = 6.00(1)\,\mu_B$ for $MnSbS_2Cl$ and $\mu_{eff} = 5.97(1)\,\mu_B$ for $MnBiS_2Cl$, within the range $5.8-6.00\,\mu_B$ corresponding to high spin Mn^{2+} [10]. Large maxima of susceptibility, characteristic of a low-dimensional anti-ferromagnetic behaviour, appear near 39 K, followed by an increase of susceptibility below 27 and 17 K, for Sb and Bi compounds, respectively.

Fig. 5 represents the evolution of magnetic susceptibility and of the specific heat versus temperature for both compounds, $MnSbS_2Cl$ and $MnBiS_2Cl$. For the Sb-bearing compound, the specific heat results show a three-dimensional (3D) long-range magnetic ordering transition at 35 K, which was not clearly visible on the magnetic susceptibility curve. For the Bi-bearing compound, a double magnetic transition with two peaks of same intensity at 28 and 32 K is distinctly observed, corresponding to a two-step magnetic transition. As both compounds are isotypic with the same quantity of Mn and their magnetic entropies are similar, this behaviour appears like an intrinsic characteristic of $MnBiS_2Cl$. Moreover, the two

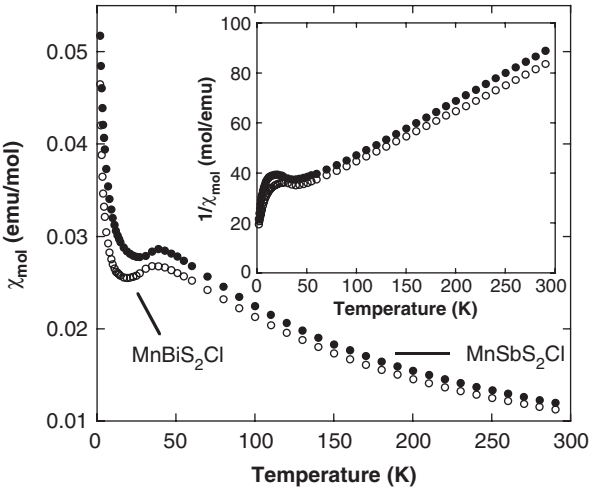

Fig. 4. Temperature dependence of the molar magnetic susceptibilities χ_{mol} of $MnSbS_2Cl$ (filled circles) and $MnBiS_2Cl$ (empty circles); the inset shows the temperature dependence of the inverse of molar susceptibility $1/\chi_{mol}$.

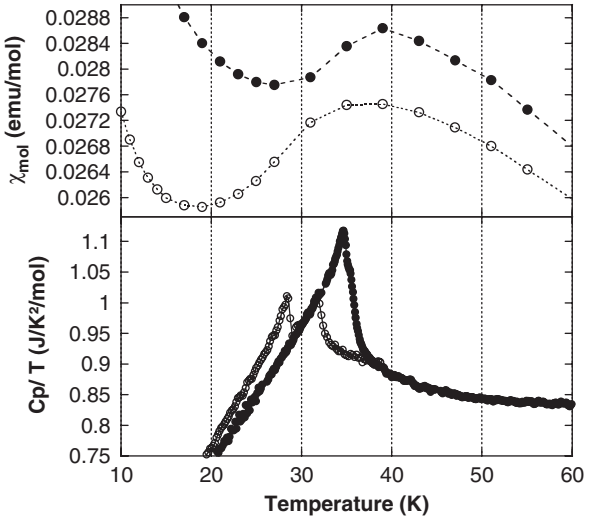

Fig. 5. Observation of the magnetic transitions by magnetic susceptibility (top) and specific heat measurements (bottom) versus temperature for $MnSbS_2Cl$ (filled circles) and $MnBiS_2Cl$ (empty circles).

peaks being of the same intensity and this one being proportional to the quantity of the phases in a mixture, there is not here 50% of impurity.

3.3. Determination of the magnetic structure of $MnSbS_2Cl$

Fig. 6 shows neutron diffraction patterns collected at 1.5 and 51 K. The neutron diffraction pattern recorded at 51 K on G4.1 for $MnSbS_2Cl$ is strictly due to the nuclear scattering with the known cell parameters $a = 9.540$, $b = 3.813$, $c = 12.224$ Å. A peak of nuclear origin, at $2\theta \sim 35^\circ$, not indexed by the nuclear phase, is due to an impurity, which could not be identified (it does not correspond to any of the by-products of the reaction, like

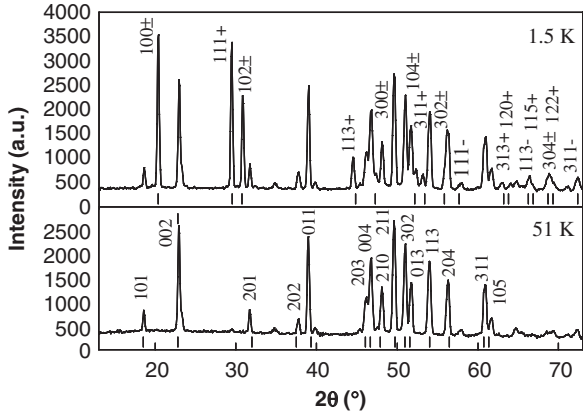

Fig. 6. Neutron diffraction patterns of $MnSbS_2Cl$ at 1.5 and 51 K. (Indexation of principal magnetic (top) and nuclear (bottom) peaks.)

MnS, $MnCl_2$ or MnO). Nevertheless, it generates no specific additional magnetic peaks at lower temperature. Additional peaks of magnetic origin appear below 35 K. Magnetic peaks observed at 1.5 K correspond to a 3D long-range magnetic ordering of the manganese magnetic moments. They can be indexed from the nuclear cell parameters using an incommensurate 1D propagation wave-vector along the b-axis, equal to $k = [0, 0.3838, 0]$. Two modulation models were tested, sinusoidal and helicoidal, giving similar magnetic reliability factors, $R_{mag} = 0.0573$ and 0.0586, respectively. The refined diagrams of both models are presented in Fig. 7. The atomic positions and magnetic moment values of manganese atoms for both modulation types are compiled in Table 4. The two possible magnetic structures are represented in Fig. 8. Manganese magnetic moments are oriented in the (a,c) plane, perpendicularly to the b-axis corresponding to the propagation wave-vector direction. Along the a-axis, as the Mn octahedra are corner-sharing, manganese atoms can enough strongly interact by a 180° super-exchange, and manganese magnetic moments are anti-ferromagnetically ordered. Along the b-axis, the edge-sharing Mn octahedra interact more weakly by a 90° super-exchange. In this direction, manganese magnetic moments follow a sinusoidal or a helicoidal modulation. The resulting magnetic moment is thus anti-ferromagnetic.

In a sinusoidal model, the manganese magnetic moments have the same direction with variable amplitudes while, in an helicoidal model, they have the same amplitude M_0 with different directions by rotation around the propagation b-axis. These two models exhibit similar magnetic reliability factors and nearly identical refined diagrams. Powder neutron diffraction measurements did not permit to choose between both. The compound $FeSb_2S_4$, berthierite [11,12], is another example of an helicoidal anti-ferromagnetic compound where the existence of a helicoidal modulation was proved by ^{57}Fe Mössbauer absorption studies.

The propagation wave-vector is constant from 1.5 to 35 K. The evolution of magnetic moment values versus temperature is represented in Fig. 9. Manganese magnetic

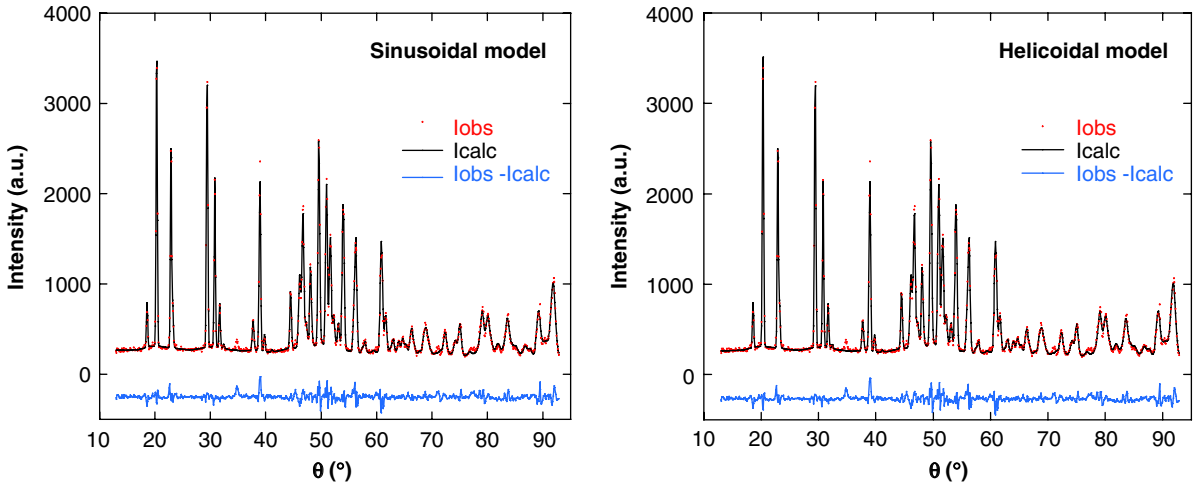

Fig. 7. Refined diagrams at 5 K of the magnetic structure of $MnSbS_2Cl$ with sinusoidal (left) or helicoidal (right) modulations.

Table 4
Atomic positions and magnetic moment values of manganese atoms for sinusoidal M_{sin} ($R_{mag} = 0.0573$) and helicoidal M_{hel} ($R_{mag} = 0.0586$) modulations of the magnetic structure of $MnSbS_2Cl$

Atom	x	y	z	$M_{sin}(x)$	$M_{sin}(y)$	$M_{sin}(z)$	M_{sin}	M_{hel}
Mn1	0.0046	0.75	0.7327	4.63(7)	0	4.38(7)	4.51(5)	4.50(3)
Mn2	−0.0046	0.25	0.2673	4.63(7)	0	4.38(7)	4.51(5)	4.50(3)
Mn3	0.5046	0.75	0.7673	−4.63(7)	0	−4.38(7)	−4.51(5)	−4.50(3)
Mn4	0.4954	0.25	0.2327	−4.63(7)	0	−4.38(7)	−4.51(5)	−4.50(3)

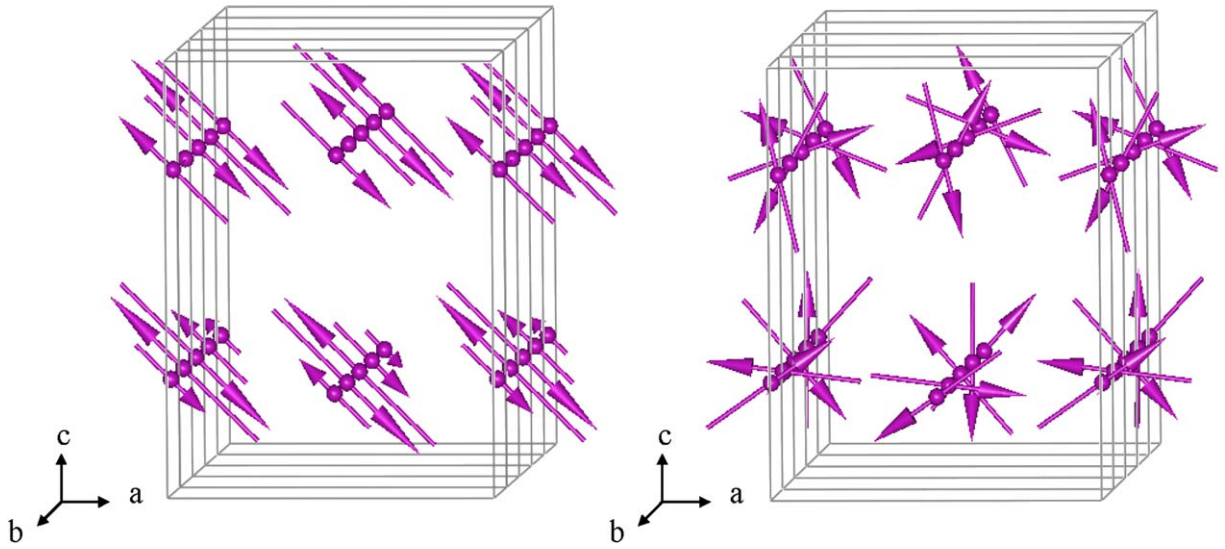

Fig. 8. Incommensurate magnetic structure of $MnSbS_2Cl$ with sinusoidal (left) or helicoidal (right) modulations.

moments have been determined from neutron diffraction patterns for each temperature. Usually, a Mn^{2+} ion in $3d^5$ high spin state is expected to have a moment close to 5 μ_B, but a maximal magnetic moment of only 4.50(3) μ_B is observed at 1.5 K (Fig. 9). The magnetic moment does not reach the expected value, due to the apparition of short-distance interactions above the magnetic transition temperature, which form a bump in the neutron patterns background between $13 < 2\theta < 35^\circ$. This character has been already observed for other compounds such as $CsNiCl_3$ [13] or jamesonite, $FePb_4Sb_6S_{14}$ [14].

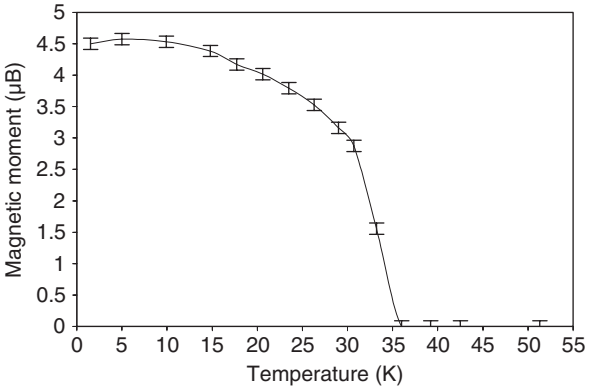

Fig. 9. Evolution of the magnetic moment (μ_B) versus temperature for $MnSbS_2Cl$.

From magnetic susceptibility and specific heat measurements, no other magnetic transition is observed at low temperature. Consequently, the susceptibility increase is inferred to a Mn impurity, corresponding to 1.8% of equivalent paramagnetic Mn^{2+}.

4. Conclusion

Both studied compounds, $MnSbS_2Cl$ and $MnBiS_2Cl$, are structurally isotypes. The Bi/Sb substitution has produced only very little changes on the susceptibility evolution and on the magnetic transition temperature. It seems very likely that the magnetic structure of Bi-bearing compound is the same than that of the Sb-bearing isotypic. Nevertheless, a double transition is clearly observed on specific heat measurements for this compound, revealing a two-step magnetic transition. The study of $MnSbS_2Cl$ by powder neutron diffraction has permitted to determine its magnetic structure which is anti-ferromagnetic with an incommensurate wave-vector. Two modulation models, sinusoidal and helicoidal, are compatible with the powder neutron diffraction data. A neutron diffraction study is planed to complete this study and determine the magnetic structure of $MnBiS_2Cl$.

References

[1] P.F. Poudeu Poudeu, T. Söhnel, M. Ruck, Z. Anorg. Allg. Chem. 630 (2004) 1276–1285.
[2] O. Tougait, J.A. Ibers, A. Mar, Acta Crystallogr. C 59 (2003) 77–78.
[3] A. Pfitzner, M. Zabel, F. Rau, Z. Anorg. Allg. Chem. 631 (2005) 1439–1441.
[4] C. Doussier, P. Léone, Y. Moëlo, Solid State Sci. 6 (2004) 1387–1391.
[5] G.M. Sheldrick, SHELXL-97, University of Göttingen, Germany, 1997.
[6] H.M. Rietveld, J. Appl. Crystallogr. 2 (1969) 65.
[7] J. Rodriguez Carvajal, Abstracts of the Satellite Meeting of the XVth Congress of the International Union of Crystallography, Toulouse, 1990, p. 127.
[8] N.E. Brese, M. O'Keeffe, Acta Crystallogr. B 47 (1991) 192–197.
[9] J. Olivier-Fourcade, A. Ibanez, J.C. Jumas, M. Maurin, I. Lefebvre, P. Lippens, M. Lannoo, G. Allan, J. Solid State Chem. 87 (1990) 366–377.
[10] R.D. Shannon, Acta Crystallogr. A 32 (1979) 751.
[11] M. Wintenberger, G. André, Physica B 162 (1990) 5.
[12] K. Lukaszewicz, A. Pietraszko, J. Stepien-Damm, A. Kajokas, J. Grigas, H. Drulis, J. Solid State Chem. 162 (2001) 79–83.
[13] V.J. Minkiewicz, D.E. Cox, G. Shirane, Solid State Commun. 8 (1970) 1001.
[14] P. Léone, G. André, C. Doussier, Y. Moëlo, J. Magn. Magn. Mater. 284 (2004) 92–96.